Fourier transform infrared spectroscopy studies of alginate–PLL capsules with varying compositions

Chris G. van Hoogmoed,[1] Henk J. Busscher,[1] Paul de Vos[2]

[1]*Department of Biomedical Engineering, Section of Bioadhesion, University of Groningen, Antonius Deusinglaan 1, 9713 AV Groningen, The Netherlands*
[2]*Departments of Pathology and Laboratory Medicine, Section of Medical Biology, Division of Immunoendocrinology, University of Groningen, Hanzeplein 1, 9700 RB Groningen, The Netherlands*

Abstract: Microencapsulation of cells is a promising approach to prevention of rejection in the absence of immunosuppression. Clinical application, however, is hampered by insufficient insight into the factors that influence the biocompatibility of the capsules. Capsules prepared of alginates with a high guluronic (G) acid content proved to be more adequate for clinical application since they are more stable, but, unfortunately, they are less biocompatible than capsules prepared of intermediate-G alginate. In order to get some insight into the physicochemical factors that influence the biocompatibility of capsules for the encapsulation of living cells, the chemical compositions of alginate–Ca beads and alginate–PLL capsules were studied by Fourier transform infrared spectroscopy. We found that during the transition of the alginate–Ca beads to alginate–PLL capsules, Ca connecting the alginate molecules, disappeared at the surface of both high-G and intermediate-G alginate–PLL capsules. At the same time, it turned out that high-G alginate–PLL capsules contained more hydrogen bonding than did intermediate-G alginate capsules. Thus the well-known higher stability of high-G alginate–PLL compared to intermediate-G alginate–PLL capsules is not caused by a higher degree of binding to Ca of the alginate molecules but rather by the presence of more hydrogen bonds. Another observation was that after the transition from bead to capsule, high-G alginate–PLL capsules contained 20% more PLL than the intermediate-G alginate–PLL capsules. Finally, we show that in both high-G and intermediate-G alginate–PLL capsules, the PLL exists in the α-helix, in the antiparallel β-sheet, and in the random coil conformation. This study shows that FT-IR allows for successful analyses of the chemical factors essential for understanding differences in the biocompatibility of alginate–PLL capsules. © 2003 Wiley Periodicals, Inc. J Biomed Mater Res 67A: 172–178, 2003

Key words: FT-IR; alginate; poly-L-lysine; encapsulation; immunoisolation

INTRODUCTION

The grafting of cells for treatment of human disorders such as hormone or protein deficiencies is limited as a consequence of having to use life-long immunosuppression in order to prevent rejection of the graft. To bypass the application of immunosuppressives, much research has been focused on the design of techniques to envelop hormone- or protein–secreting cells in semipermeable membranes in order to protect donor cells against antibodies and cytotoxic cells within the host immune system. Such immunoprotection by encapsulation allows not only for successful transplantation of cells in the absence of immunosuppression[1–3] but also for transplantation of cells of non-human origin, that is, xenografts. The use of xenografts, of course, is highly desirable because of the limited supply of donor tissue. Because of these benefits, the feasibility of transplanting cells in immunoprotective membranes is under study for the treatment of a wide variety of endocrine diseases.[4–8]

A commonly used procedure for immunoprotection is microencapsulation of tissues in alginate–poly-L-lysine (PLL)-based capsules, as originally described by Lim and Sun.[3] During recent years, important advances have been made with this technology. The first allotransplantations in humans with encapsulated parathyroid cells and islets have been successfully performed.[9,10] Although this illustrates the principal applicability of the alginate-encapsulation technique, a fundamental barrier still must be overcome since graft survival varies considerably from several days to months.[1,11–13] This variation in success rate usually is

attributed to differences in chemical composition[14–17] and thus to differences in the biocompatibility of the applied capsules.

The formation of adequate capsules for successful transplantation is far from simple and to date poorly standardized. Many factors that are difficult to control in a conventional laboratory, such as environmental temperature and differences in alginate composition, have major consequences for the chemical characteristics of the capsules and thus the outcome of the graft.

Fourier transforming-infrared spectroscopy (FT-IR) is a technique that allows for characterization of structural features of complex polymeric materials and biofilms.[18–20] FT-IR also is used often for detailed study of intramolecular and intermolecular interactions. Such an approach also may serve as a technique for testing and controlling the formation of alginate–PLL capsule formation as it can, theoretically, characterize the chemistry of capsules in a detailed fashion and detect small but essential differences in capsular composition. In the present study we have tested the efficacy of Fourier transforming-infrared spectroscopy as a method for assessing the adequacy of alginate–PLL capsule formation. To this end, we report and compare FT-IR spectra of high- and intermediate-G Ca beads coated with PLL.

MATERIALS AND METHODS

Alginates

Alginates contain various amounts of guluronic-acid (G) chains and mannuronic-acid (M) chains (G/M ratio). Intermediate-G (Keltone LV) and high-G (Manugel) sodium alginates were obtained from Kelco International (London). Purification of alginate was performed as described in detail elsewhere.[1] The alginates were dissolved at 4°C in Krebs-Ringer-Hepes (KRH) with an appropriate osmolarity to a solution with a viscosity of 4 cps. This viscosity is necessary for the production of spheric droplets without any tails or other imperfections associated with bioincompatibility. The viscosity of an alginate solution is determined by the concentration of the alginate, but different alginates have different viscosities. This implies for the intermediate-G (i.e., low viscosity) solution a concentration of 3% and for the high-G solution a 2% concentration to obtain a viscosity of 4 cps. The solutions were sterilized by 0.2-μm filtration.

Microencapsulation

Alginate solutions were converted into droplets using an air-driven droplet generator, as previously described.[21] Briefly, the alginate droplets were transformed to alginate beads by gelling in a 100-mM CaCl$_2$ (10 mM of HEPES, 2 mM of KCl) solution for at least 5 min. After gelation the beads had a diameter of 450–550 μm. Subsequently, the Ca–alginate beads were suspended for 1 min in KRH containing 2.5 mmol/L of CaCl$_2$. A poly-L-lysine (PLL) membrane was formed by suspending the alginate beads in 0.1% PLL solution for 10 min (poly-L-lysine-HCl, Mw: 22,000, Sigma). This produces capsules that are impermeable for substances above 100 kD.[22]

Non-bound PLL was removed by three successive washings within 3 min with Ca^{2+}-free KRH containing 135 mM of NaCl. The outer alginate layer subsequently was applied by 5 min of incubation in 10-times-diluted alginate solution. Finally, the capsules had a diameter of 600–700 μm. All procedures were performed under sterile conditions.

Fourier transforming-infrared spectroscopy (FT-IR)

For FT-IR analyses, beads and capsules were washed three times with ultrapure water and gradually lyophilized (Leybold Herecuis, Combitron CMI). It is a prerequisite that the membranes of the capsules be intact and not broken.[15] Therefore, before applying FT-IR, we confirmed the integrity of the surfaces and membranes both at low magnification (i.e., by light microscopy) and at high magnification (i.e., by scanning electron microscopy).

Infrared absorption spectra were recorded on a FTS-175 spectrometer from Bio-Rad Laboratories (USA) with a spectral resolution and a wave-number accuracy of 4 cm^{-1} and 0.01 cm^{-1}, respectively. The spectrometer was equipped with a Golden Gate Single Reflection Diamond ATR. For measurements, beads or capsules were put centrally on the diamond. With a top clamp mechanism, fitted with a flat sapphire anvil, the sample was compressed between the sapphire and the diamond anvil. A working pressure of 70 cNm was used.

Before the spectra of the samples were recorded, the sample compartment was flushed with N$_2$ gas to prevent disturbance by water and CO$_2$. All measurements consisted of 200 scans, using the bare diamond anvil as background. All presented spectra were means based on corrected data for water and CO$_2$ from three measurements with separately prepared samples. Fourier self-deconvolution was done with an exponential filter, which tends to sharpen spectral features. To reduce the apparent noise in the data correlated with Fourier self-convolution, a smoothing filter simultaneously was applied without losing peak resolution.

RESULTS

Spectroscopic analyses of the alginate–Ca beads and the alginate–PLL capsules were based on three distinct frequency regions. The first region involves proteins (1700–1480 cm^{-1}) with bands centered near 1640 cm^{-1} and 1530 cm^{-1}, corresponding, respectively, to υ C=O + υ C—N + δ N—H (amide I) and δ N—H + υ C—N (amide II) of the peptide bond. The second is the carbohydrate region (1200–870 cm^{-1}), with a main peak near 1029 cm^{-1}, which originates from the cou-
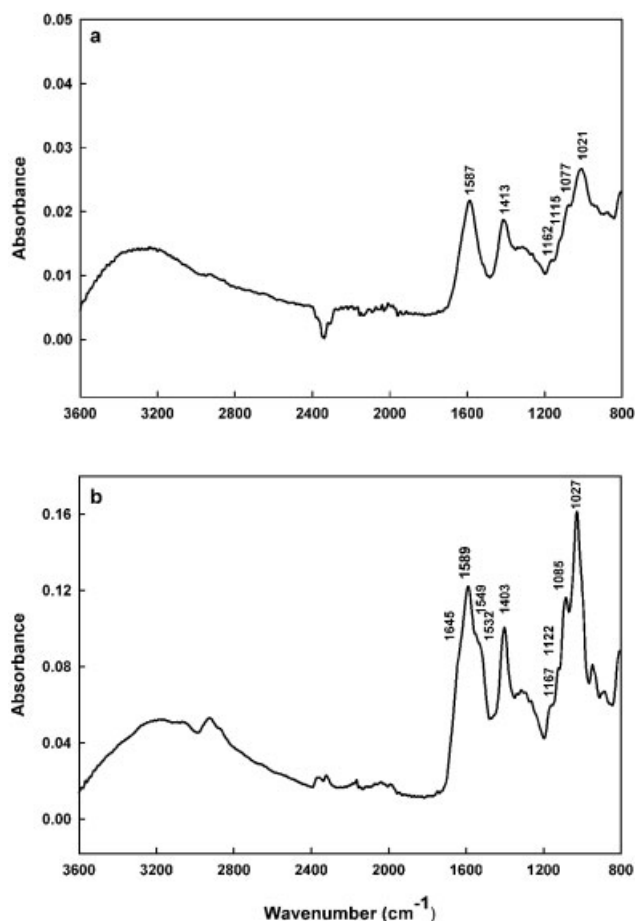
Figure 1. FT-IR spectra of (a) high-G alginate–Ca beads and (b) high-G alginate–PLL capsules.

pling of the υ C—O + υ C—C + δ C—O—H vibrations. The third region is that of the υ O—H, υ N—H, υ C—H, and the υ C—H$_2$ bands (3500–2850 cm^{-1}).

In general, the FT-IR spectrum of intermediate-G Ca beads is comparable with the FT-IR spectrum of high-G Ca beads, as shown in Figure 1(a). Ca beads show characteristic bands in the carbohydrate region. Also some specific Ca beads' bands were observed in the asymmetric stretching band of the COO$^-$ group near 1590 cm^{-1} (υ_a COO$^-$), and the symmetric stretching band of the COO$^-$ group centered near 1410 cm^{-1} (υ_s COO$^-$).

The changes in the FT-IR spectra associated with the transition of Ca beads to alginate–PLL capsules are presented in Figure 1(a,b). The measured frequencies of the bands are presented in Table I. This is done for Ca beads and capsules prepared from both intermediate-G and high-G alginate. The changes in the different regions when Ca beads are transformed into capsules will be discussed in the following sections.

Carbohydrate-absorption-region-associated changes

The transition from high-G and intermediate-G Ca beads to capsules resulted in frequency shifts in the carbohydrate region, especially in the 1170–1020 region. Frequency displacements took place for intermediate-G Ca bead bands at 1165, 1123, 1080, and 1026 cm^{-1}, which were upshifted, respectively, to 1169, 1124, 1083, and 1029 cm^{-1} in the intermediate-G capsules. The high-G Ca beads were upshifted from 1162, 1121, 1080, and 1020 cm^{-1} to 1163, 1124, 1085, and 1029 cm^{-1}, respectively, in the high-G capsules. These bands are identified and presented in Table I. Although not considered statistically significant, we found a more pronounced upshift with high-G alginate than with intermediate-G alginate.

Protein-absorption-region-associated changes

The coating of the high and intermediate-G Ca beads with PLL resulted in the formation of the amide I and amide II bands for alginate–PLL capsules. These amide I and amide II bands were visible only as weak shoulders on the broad υ_a COO$^-$ band [Fig. 1(b)]. The amide I band was located at 1645 cm^{-1}, and for amide II, two bands were observed, at 1549 and 1532 cm^{-1}. Intermediate-G alginate–PLL capsules showed the same results for the amide bands as did high-G alginate–PLL capsules (not shown in Fig.1).

Upon zooming in on the protein region for intermediate-G and high-G capsules, more weak shoulders were visible. To study these protein bands in greater detail, the protein regions for intermediate-G and high-G capsules were deconvoluted, as shown in Figure 2(a,b), respectively. After deconvolution, the weak shoulders at 1645 cm^{-1} (amide I) and at 1549 and 1532 cm^{-1} (amide II) were clearly discernable for both high-G and intermediate-G alginate–PLL capsules. We found clear bands as shoulders at 1691, 1680, 1669, 1658, 1625, 1607, 1568, and 1522 cm^{-1}.

These shoulders, with the exceptions of the frequencies at 1607 and 1522, which are representative for δ_a NH$_3^+$ and δ_s NH$_3^+$, represent conformational structures of the bound PLL. The shoulder at 1658 cm^{-1} is representative of the α-helix conformation; the shoulders at 1691, 1625, 1568, and 1532 cm^{-1} are representative of the antiparallel β-sheet conformation; and the shoulders at 1654 and 1549 cm^{-1} are representative of the random coil formation of PLL.

In addition to the protein absorption bands the υ_s COO$^-$ band also is present in this region. This band was downshifted with about 10 cm^{-1} for both intermediate- and high-G capsules during the transition from beads to capsules (Table I).

The υO—H, the υN—H, the υC—H, and the υC—H$_2$ region

Figure 3 shows the O—H and N—H stretching region (3000–3500 cm^{-1}). The band in this region was

TABLE I
FT-IR Absorption Bands (cm^{-1}) of Intermediate-G and High-G alginate Ca Beads and PLL Capsules

Intermediate-G Alginate		High-G Alginate		
Ca Beads	Alginate–PLL Capsules	Ca Beads	Alginate–PLL Capsules	Assignment
	3060		3062	νNH
	2929		2927	ν_a(CH$_2$)
	2892			ν (CH)
	2868		2873	ν_s(CH$_2$)
	2835			
	1643		1643	Amide I
1587	1590	1587	1589	ν_s (COO$^-$)
	1549		1549	Amide II
	1532			
1410	1401	1412	1403	ν_a (COO$^-$)
1339	1339	1337	1337	
1315	1313	1314	1315	δ (OH), δ (CH), τ (CH),
1299	1293		1294	w (CH).
1262	1262	1263	1262	
1165	1169	1162	1163	ν (COC), ν (OH)
1123	1124	1121	1124	ν (CO), ν_s (CC)
1080	1083	1080	1085	ν (CO), δ (CCO), δ (CC)
1026	1029	1020	1029	ν (CO), ν (CC), δ (COH)
1009		1009		
	947		947	
930	935	933	932	
883	885	874	884	
807	808	809	807	

ν: stretching; δ: bending; τ: twisting; w: wagging; s: symmetric; a: asymmetric.

for the beads caused by O—H stretching only and was virtually the same for intermediate-G and high-G beads. After coating the beads with PLL, the νNH band originated at different places for the two types of alginates; that is, for intermediate-G capsules it originated at 3060 cm^{-1}, and for high-G capsules it originated at 3062 cm^{-1} (see Table I). Also the transition from bead to capsule induced a broadening towards frequencies lower than 3000 cm^{-1} and towards a higher intensity of the O—H and N—H stretching band for both high-G and intermediate-G capsules. This broadening and higher intensity was greater during the preparation of high-G capsules.

PLL contains methylene groups. In infrared spectra the methylene groups show asymmetric stretching (ν_a CH$_2$) near 2925 cm^{-1} and symmetric stretching (ν_s CH$_2$) near 2850 cm^{-1}. Concomitantly, with the PLL coating of the Ca beads, methylene groups are introduced in the high-G and intermediate-G alginate–PLL capsules.

The methylene groups also can serve as a measure to quantify the PLL content of alginate–PLL capsules since PLL is the only component of the capsules containing methylene groups. As shown in Figure 3, absorptions associated with ν_a CH$_2$ and ν_s CH$_2$ in high-G capsules were located, respectively, at 2920 and 2868 cm^{-1}, and those for intermediate-G capsules were located, respectively, at 2924 and 2863 cm^{-1}.

Furthermore, the methylene absorption bands present in the spectrum of the high-G capsules were more abundant. To quantify and compare the lysine content of high-G and intermediate-G alginate–PLL capsules, the surface areas of the ν_a CH2 band for high-G and the intermediate-G capsules were normalized with respect to the surface area of the ν_s COO$^-$ band around 1400 cm^{-1}. This procedure yielded a ν_a CH$_2$/ν_s COO$^-$ ratio of 1.7 for high-G capsules and a ration of 1.4 for intermediate-G capsules. This implies that high-G capsules contain 20% more PLL than do intermediate-G capsules.

DISCUSSION

In the present FT-IR study, the spectrometer was equipped with a Golden Gate single reflection diamond ATR. Because of the size of the studied beads and capsules, the penetration depth of the radiation from this infrared reflectance technique (4.4 μm at 1000 cm^{-1}) is many times smaller than the diameter of the beads and capsules. It is reasonable to assume, therefore, that in this study the surface of the beads and capsules was analyzed.

It has been shown that high-G alginates have some advantages over intermediate-G alginates for application in cell encapsulation. It has been shown in *in vitro* studies that capsules prepared of high-G alginates have a higher mechanical stability than capsules prepared of intermediate-G alginate.[14,15,23,24] Also they con-
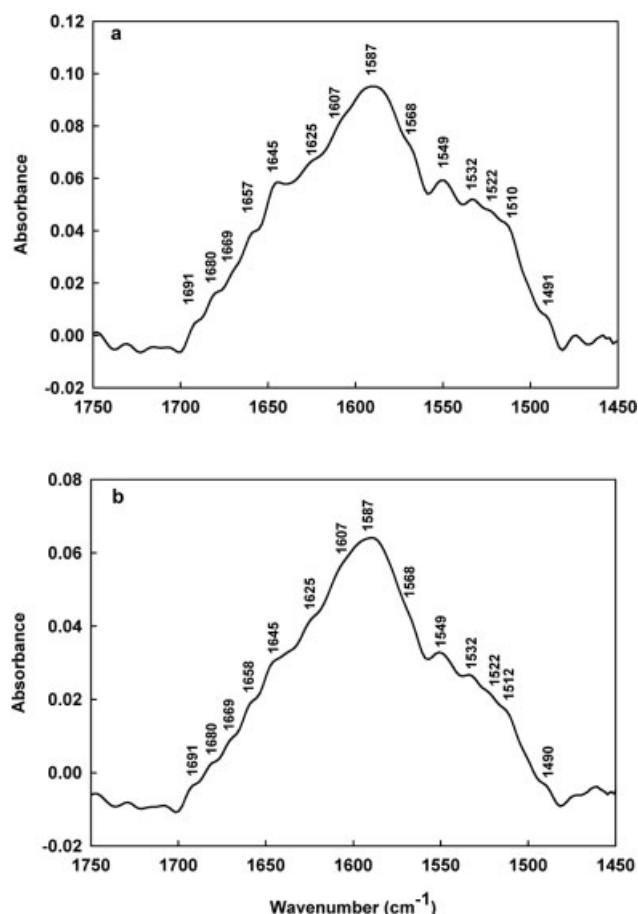
Figure 2. FT-IR spectra of the protein region for (a) intermediate-G and (b) high-G alginate–PLL capsules following Fourier transform self-deconvolution.

tain much lower numbers of incompletely, and therefore inadequately, encapsulated cells.[22,25] Unfortunately, an *in vivo* study by our group showed that after transplantation in rats, the majority of high-G capsules are overgrown by inflammatory cells and are adherent to the abdominal organs whereas with intermediate-G alginate, most capsules are floating freely in the peritoneal cavity and are free of any cell adhesion.[14,16]

A recent X-ray photoelectron spectroscopy study by de Vos et al.[15] show a correlation of these biologic responses with the chemical compositions of the capsule surfaces. The authors observed that high-G alginate capsules have too high a content of PLL. Our present FT-IR study confirms these observations since in the present study we found a 20% higher PLL content in high-G capsules than in intermediate-G capsules.

The formation of Ca beads is accomplished by diffusion into the alginate network of calcium. As a consequence of Ca diffusion into the alginate network, the νC—O and the δC—O—H vibrations shift to lower frequencies,[26] and spectral changes in the regions of the COO⁻ antisymmetric and symmetric stretching vibrations occur.[27]

During the transition of Ca beads to capsules, PLL diffuses into the network of alginate crosslinked with Ca. After this process, frequency upshifts of the bands in the carbohydrate region (1170–1020 cm^{-1}), to which the νC—O and the δC—O—H vibrations also belong, were observed (Table I). This upshift is associated with the disappearance of Ca. Our results also showed that this upshift is influenced by the type of alginate since high-G alginate beads showed the highest upshifts, suggesting that more Ca in high-G alginate disappears than is the case in intermediate-G alginate.

Another shift associated with the disappearance of Ca is the observed downshifting of the ν_s COO⁻, with 10 cm^{-1} (Table I) for both the intermediate-G and the high-G alginate.

Because of its high affinity for G blocks (i.e., G residues), Ca connects two alginate molecules by binding to the consecutive G blocks located on each of the two molecules[28,29] in a cooperative manner. Since high-G alginate contains more G blocks than intermediate-G alginate, it is generally assumed that this is the major cause for the well-known higher stability of capsules prepared with high-G alginate.[23,24,30] Despite the observed disappearance in this study of Ca, the capsules of high-G alginate retained their stability.

An explanation for the retained stability is hydrogen bonding, illustrated by a broadening towards frequencies lower than 3000 cm^{-1} and an intensity increase of the O—H and N—H stretching band after the conversion of beads to capsules for both high-G and intermediate-G alginates (Fig. 3). However, the most dramatic changes were observed for high-G alginate, suggesting that high-G alginate capsules contain more hydrogen bonding, which leads to more stable capsules.
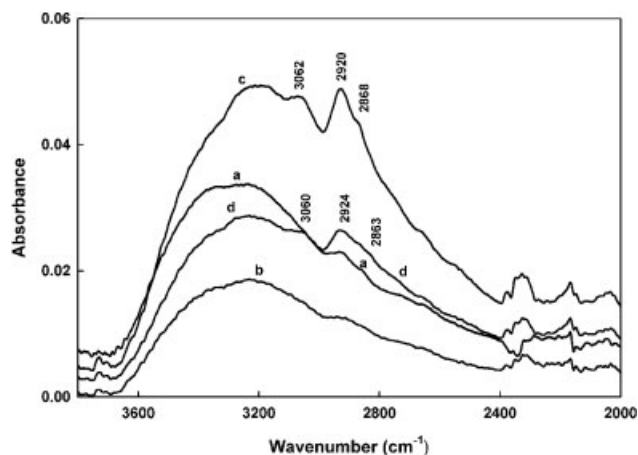

Figure 3. FT-IR spectra of the 2000–3700 cm^{-1} region with the O—H stretching vibrations for (a) high-G Ca beads and (b) intermediate-G Ca beads and the O—H, N—H ($\pm$ 3060 cm^{-1}), and C—H$_2$ ($\pm$ 2922 cm^{-1} and $\pm$ 2866 cm^{-1}) stretching vibrations for (c) high-G alginate–PLL capsules and (d) intermediate-G alginate–PLL capsules.
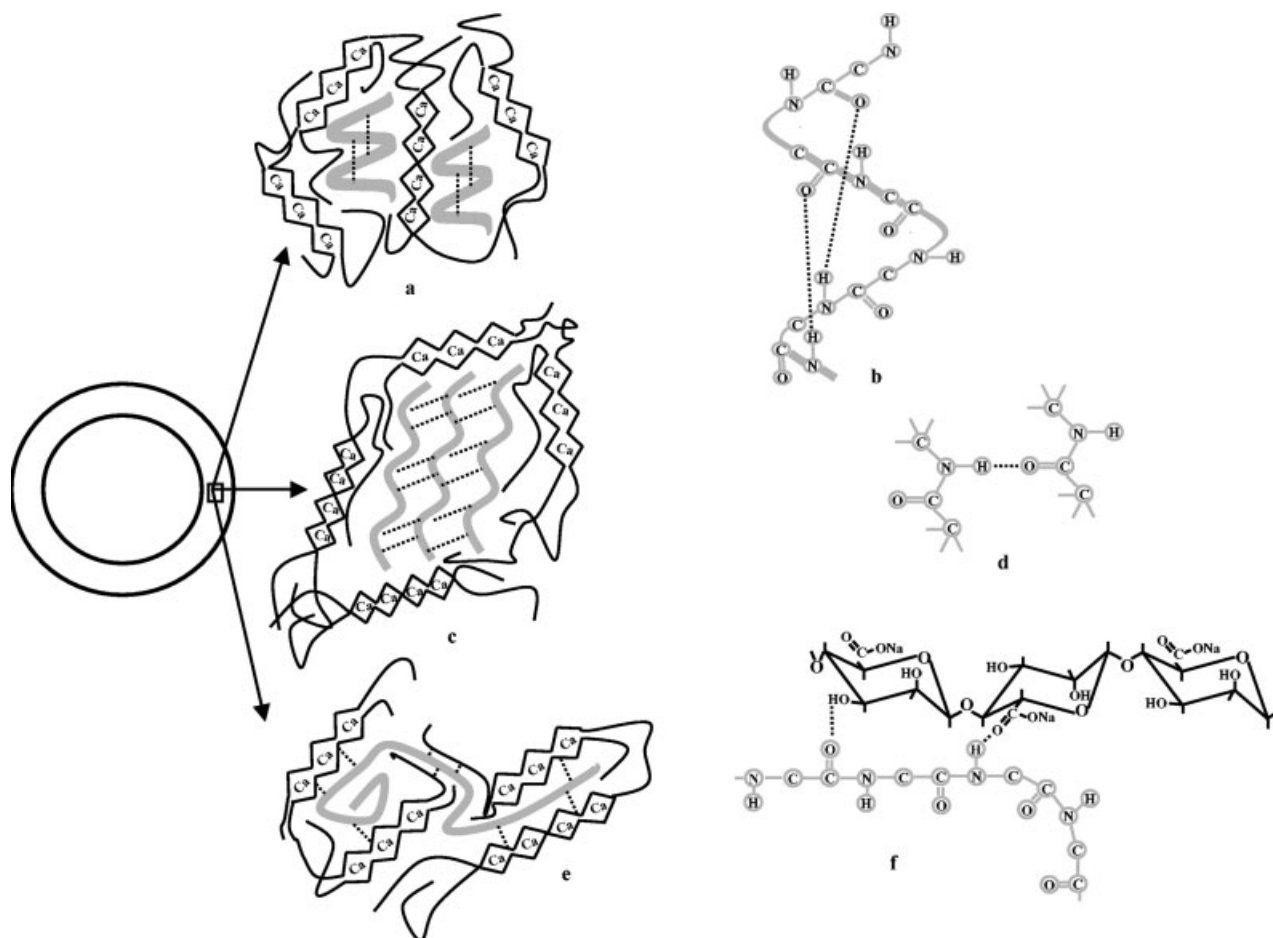
Figure 4. The composition of the alginate–PLL membrane of high-G and intermediate-G capsules. Protein and alginate structures are, respectively, gray and black colored. (a) The α-helical structure of PLL derived from formation of (b) intramolecular hydrogen bonding between amide groups, (c) the antiparallel β-sheet structure of PLL derived from formation of (d) intermolecular hydrogen bonding between amide groups of different PLL chains, and (e) a random coil formation of PLL due to (f) hydrogen bonding between PLL and alginate molecules. The dotted lines (- - - -) represent hydrogen bonds.

Recently it has been shown by de Vos et al.,[15] by applying XPS, that high-G capsules have fewer binding sites for PLL than do intermediate-G capsules. In the present study we observed that the presence of fewer binding sites for PLL is not an obstacle for PLL to diffuse in higher amounts and to interact with the alginate molecules, with more hydrogen bonds being formed in the high-G alginate beads than in the intermediate-G alginate beads.

This phenomenon can be explained by the difference in pore size between high-G and intermediate-G Ca beads. The pores of high-G alginate beads are larger than those of intermediate-G beads, and larger pores allow a higher PLL uptake.[23,24] Because of greater hydrogen bonding in high-G alginate, it is plausible that the binding sites present in high-G alginate are very accessible for PLL. This is in contrast with a larger number of binding sites for PLL but less hydrogen bonding in intermediate-G alginate.

It has been shown that high-G capsules provoke pronounced inflammatory reactions when implanted in the peritoneal cavity of rats.[14] The following mechanism may be involved: A large amount of PLL is diffused into the high-G alginate beads. As a consequence of the limited number of binding sites in high-G alginate, not all PLL molecules, or only parts of the long PLL molecules, will have interactions with the high-G alginate. Since there are fewer interactions between parts of the alginate and PLL in high-G capsules it is quite conceivable that some PLL diffuses out of the capsules after implantation and induces an inflammatory response. PLL is a well-known inducer of inflammatory responses when inadequately bound to alginate.[17,31]

Our study provides new insight into the chemical structure of PLL in the capsule membranes. PLL as a sole molecule can exist in the α-helix, the random coil, and the antiparallel β-sheet conformation (see Fig. 4). After having applied FT-IR on a solution of a mixture of PLL and alginate, Dupuy et al.[18] concluded that PLL forms a random coil in the presence of alginate. Our present observations do not corroborate this explanation since with true capsules, instead of sole molecules, we found in the deconvoluted protein regions of high-G and intermediate-G capsules [Fig.

2(a,b)], in addition to the random coil conformation, the frequencies for the α-helix and the antiparallel β-sheet conformation. This implies that PLL exists in different conformations in the alginate capsules.

It is plausible that when sufficient interactions are possible between PLL and alginate molecules, PLL forms random coil formations [Fig. 4(e,f)]. In the absence of sufficient interactions between PLL and alginate molecules, PLL may form hydrogen bonds only intramolecularly, which would lead to the α-helix [Fig. 4(a,b)] and antiparallel β-sheet [Fig. 4(c,d)] conformation of PLL.

Intermediate-G capsules allow for successful transplantation of allogenic pancreatic islets[1,25] while high-G capsules are associated with failure due to insufficient biocompatibility.[14]

The present study demonstrates the efficacy of FT-IR for analysis of the pivotal factors for producing biocompatible capsules. We show, for the first time, that FT-IR successfully allows for analyses of the protein content and of the strength and type of interactions between PLL and alginate in true capsules. These factors are pertinent and determine the success or failure of the capsules.

References

1. De Vos P, De Haan BJ, Wolters GHJ, Strubbe JH, Van Schilfgaarde R. Improved biocompatibility but limited graft survival after purification of alginate for microencapsulation of pancreatic islets. Diabetologia 1997;40:262–270.
2. De Vos P, van Straaten JF, Nieuwenhuizen AG, de Groot M, Ploeg RJ, De Haan BJ, Van Schilfgaarde R. Why do microencapsulated islet grafts fail in the absence of fibrotic overgrowth? Diabetes 1999;48:1381–1388.
3. Lim F, Sun AM. Microencapsulated islets as bioartificial endocrine pancreas. Science 1980;210:908–910.
4. Aebischer P, Russell PC, Christenson L, Panol G, Monchik JM, Galletti PM. A bioartificial parathyroid. Am Soc Artif Intern Org Trans 1986;32:134–137.
5. Chang PL, Shen N, Westcott AJ. Delivery of recombinant gene products with microencapsulated cells in vivo. Hum Gene Ther 1993;4:433–440.
6. Koo J, Chang TSM. Secretion of erythropoietin from microencapsulated rat kidney cells. Int J Artif Org 1993;16:557–560.
7. Liu HW, Ofosu FA, Chang PL. Expression of human factor IX by microencapsulated recombinant fibroblasts. Hum Gene Ther 1993;4:291–301.
8. Wong H, Chang TM. Bioartificial liver: Implanted artificial cells microencapsulated living hepatocytes increases survival of liver failure in rats. Int J Artif Org 1986;9:335–336.
9. Hasse C, KlÖck G, Schlosser A, Zimmermann U, Rothmund M. Parathyroid allotransplantation without immunosuppression. Lancet 1997;350:1296–1297.
10. Soon Shiong P, Heintz RE, Merideth N, Yao QX, Yao Z, Zheng T, Murphy M, Moloney MK, Schmehl M, Harris M. Insulin independence in a type 1 diabetic patient after encapsulated islet transplantation. Lancet 1994;343:950–951.
11. KlÖck G, Frank H, Houben R, Zekorn T, Horcher A, Siebers U, WÖhrle M, Federlin K, Zimmermann U. Production of purified alginates suitable for use in immunoisolated transplantation. Appl Microbiol Biotechnol 1994;40:638–643.
12. Sun YL, Ma XJ, Zhou DB, Vacek I, Sun AM. Normalization of diabetes in spontaneously diabetic cynomologus monkeys by xenografts of microencapsulated porcine islets without immunosuppression. J Clin Invest 1996;98:1417–1422.
13. Zekorn T, Siebers U, Horcher A, Schnettler R, KlÖck G, Bretzel RG, Zimmermann U, Federlin K. Barium–alginate beads for immunoisolated transplantation of islets of Langerhans. Transplant Proc 1992;24:937–939.
14. De Vos P, De Haan B, Van Schilfgaarde R. Effect of the alginate composition on the biocompatibility of alginate–polylysine microcapsules. Biomaterials 1997;18:273–278.
15. De Vos P, Van Hoogmoed CG, Busscher HJ. Chemistry and biocompatibility of alginate–PLL capsules for immunoprotection of mammalian cells. J Biomed Mater Res 2002;60:252–259.
16. De Vos P, Van Schilfgaarde R. Biocompatibility issues. In: Kühtreiber WM, Lanza RP, Chick WL, editors. Cell encapsulation technology and therapeutics. Boston: Birkhäuser; 1999. p 63–79.
17. Vandenbossche GM, Bracke ME, Cuvelier CA, Bortier HE, Mareel MM, Remon JP. Host reaction against empty alginate–polylysine microcapsules. Influence of preparation procedure. J Pharmaceut Pharmacol 1993;45:115–120.
18. Dupuy B, Arien A, Perrot Minnot A. FT-IR of membranes made with alginate–polylysine complexes. Variations with mannuronic or guluronic content of the polysaccharides. Artif Cells, Blood Subs, Immob Biotech 1994;22:71–82.
19. Lamberti FV, Sefton MV. FT-IR measurement of emulsified cationic DMAEMA–MMA adsorption to calcium alginate. Biomaterials 1992;13:1109–1115.
20. Nivens DE, Ohman DE, Williams J, Franklin MJ. Role of alginate and its O acetylation in formation of *Pseudomonas aeruginosa* microcolonies and biofilms. J Bacteriol 2001;183:1047–1057.
21. De Vos P, De Haan BJ, Van Schilfgaarde R. Upscaling the production of encapsulated islets. Biomaterials 1997;18:1085–1090.
22. De Vos P, De Haan BJ, Wolters GHJ, Van Schilfgaarde R. Factors influencing the adequacy of microencapsulation of rat pancreatic islets. Transplantation 1996;62:888–893.
23. Thu B, Bruheim P, Espevik T, Smidrod O, Soon-Shiong P, Skjåk-Braek G. Alginate polycation microcapsules. I. Interaction between alginate and polycation. Biomaterials 1996;17:1031–1040.
24. Thu B, Bruheim P, Espevik T, Smidrod O, Soon-Shiong P, Skjåk-Braek G. Alginate polycation microcapsules II. Some functional properties. Biomaterials 1996;17:1069–1079.
25. De Vos P, De Haan BJ, Pater J, Van Schilfgaarde R. Association between capsule diameter, adequacy of encapsulation, and survival of microencapsulated rat islet allografts. Transplantation 1996;62:893–899.
26. Kodad H, Mokhlisse R, Davin E, Mille G. Etude des interactions sucre-cation en solution aqueuse par spectroscopie IRTF. Can J Analyt Sci Spectrosc 1998;43:129–136.
27. Nara M, Tasumi M, Tanokura M, Hiraoki T, Yazawa M, Tsutsumi A. Infrared studies of interaction between metal ions and Ca^{2+}-binding proteins. Marker bands for identifying the types of coordination of the side-chain COO^- groups to metal ions in pike parvalbumin (pI = 4.10). FEBS Lett 1994;349:84–88.
28. Skjåk-Braek G, Martinsen A. Applications of some algal polysaccharides in Biotechnology. In: Guiry MD, Blunden G, editors. Seaweed resources in Europe: Uses and potentials. New York: Wiley; 1991. p 219.
29. Smidsrod O, Skjåk-Braek G. Alginate as immobilization matrix for cells. Trends Biotechnol 1990;8:71–78.
30. Thu B, Skjåk-Braek G, Micali F, Vittur F, Rizzo R. The spatial distribution of calcium in alginate gel beads analysed by synchrotron-radiation induced X-ray emission (SRIXE). Carbohydrate Res 1997;297:101–105.
31. Strand BK, Ryan L, In 't Veld P, Kulseng B, Rokstad AM, Skjåk-Braek G, Espevik T. Poly-L-lysine induces fibrosis on alginate microcapsules via the induction of cytokines. Cell Transplant 2001;10:263–277.